New Polyketides from the Marine-Derived Fungus *Letendraea* Sp. 5XNZ4-2

Yan Xu [1], Ruibao Huang [1], Hongwei Liu [2], Tingting Yan [1], Wanjing Ding [1], Yongjun Jiang [1], Pinmei Wang [1], Daoqiong Zheng [1] and Jinzhong Xu [1,*]

[1] Ocean College, Zhoushan Campus, Zhejiang University, Zhoushan 316021, China; xuyan875@126.com (Y.X.); fau_rhuang@fau.edu (R.H.); ytt706@126.com (T.Y.); wading@zju.edu.cn (W.D.); yongjunjiang89@hotmail.com (Y.J.); wangpinmei@zju.edu.cn (P.W.); zhengdaoqiong@zju.edu.cn (D.Z.)

[2] State Key Laboratory of Mycology, Institute of Microbiology, Chinese Academy of Sciences, Beijing 100101, China; liuhw@im.ac.cn

* Correspondence: xujinzhong@zju.edu.cn; Tel.: +86-158-5816-8018

Abstract: Marine-derived fungi have been reported to have great potential to produce structurally unique metabolites. Our investigation on secondary metabolites from marine-derived fungi resulted in the isolation of seven new polyketides (phomopsiketones D–G (**1**–**4**) and letendronols A–C (**5**–**7**)) as well as one known xylarinol (**8**) in the cultural broth of *Letendraea* sp. Their structures and absolute configurations were elucidated using a set of spectroscopic and chemical methods, including HRESIMS, NMR, single-crystal X-ray diffraction, ECD calculation, and a modified version of Mosher's method. Compound **2** showed weak inhibition against nitric oxide production in lipopolysaccharide-activated macrophages with an IC_{50} value of 86 μM.

Keywords: marine-derived fungus; Letendraea sp.; polyketide; phomopsiketone; letendronol

1. Introduction

Metabolites from marine-derived microorganisms have become important pharmacological resources [1,2]. At least 2000 novel natural products have been identified in the past five years, nearly 50% of which were derived from marine-derived fungi [3–5]. In addition, the metabolic pathways of marine-derived fungi, which can be attributed to unique marine habitats, especially those that contain sea salts, may be significantly different from terrestrial ones [6]. Thus, marine-derived fungi have great potential to produce structurally unique metabolites and have attracted a considerable amount of attention.

In our ongoing research on bioactive secondary metabolites from marine-derived fungi, we isolated an endophytic fungus *Letendraea* sp. 5XNZ4-2 from one sea crab. We obtained two novel spiroketals (letenketals A and B) from this fungus [7]. In order to obtain more structurally novel compounds, the systematic discovery of secondary metabolites for this strain was carried out. Seven new polyketides (phomopsiketones D–G (**1**–**4**) and letendronols A–C (**5**–**7**), see Figure 1) as well as one known xylarinol (**8**) were isolated from a Potato DFextrose Broth (1/2 PDB) cultural broth. Herein, we report the isolation, structure elucidation, and bioactivities of these compounds.
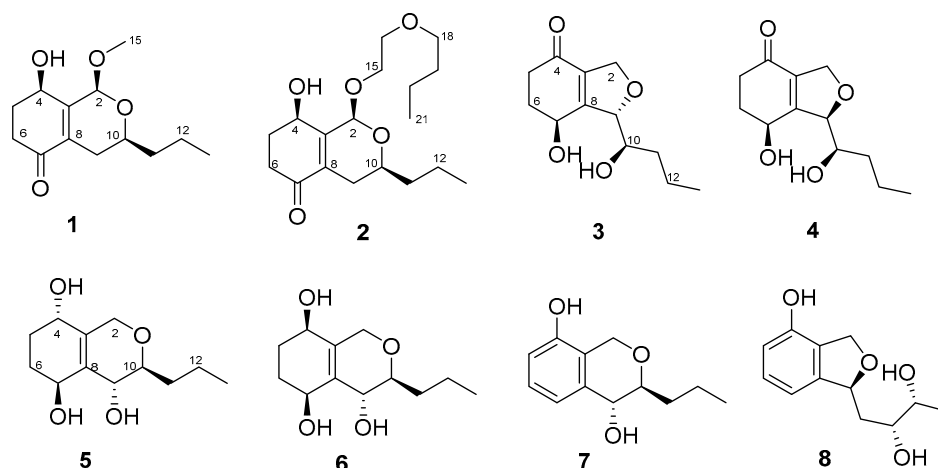
Figure 1. Chemical structures of compounds **1–8** isolated from *Letendraea* sp. 5XNZ4-2.

2. Results and Discussion

Compound **1** was obtained as a yellow amorphous powder. Its molecular formula was determined to be $C_{13}H_{20}O_4$ (with 4 degrees of unsaturation) by HRESIMS (*m/z* 263.1256 for [M+Na]$^+$) and NMR data. IR absorption at 3426 and 1672 cm^{-1} indicated the presence of a hydroxyl and unsaturated ketones. ^{1}H-NMR (Table 1) of **1** displayed one methoxy (δ_H 3.50, s) and one methyl (δ_H 0.95, t, *J* = 7.0 Hz). The ^{13}C NMR and DEPT displayed 13 carbon signals, including one α, β- unsaturated ketone (δ_C 198.2), two olefinic carbons (δ_C 132.5, 151.4), one ketal carbon (δ_C 95.2), two oxygenated carbons (δ_C 65.3, 66.7), and one methoxy (δ_C 55.8). Calculation of unsaturation revealed that compound **1** contained a bicyclic skeleton. An α, β-unsaturated cyclohexanone moiety was derived from the ^{1}H-^{1}H Correlation Spectroscopy (COSY) correlations between H-4 (δ_H 4.59)/H$_2$-5 (δ_H 2.06, 2.28)/H$_2$-6 (δ_H 2.40, 2.70), coupled with the Heteronuclear Multiple Bond Correlation (HMBC) correlations from H$_2$-5 to C-3 (δ_C 151.4) and C-7 (δ_C 198.2) and H$_2$-6 to C-7 and C-8 (δ_C 132.5) (Figure 2).
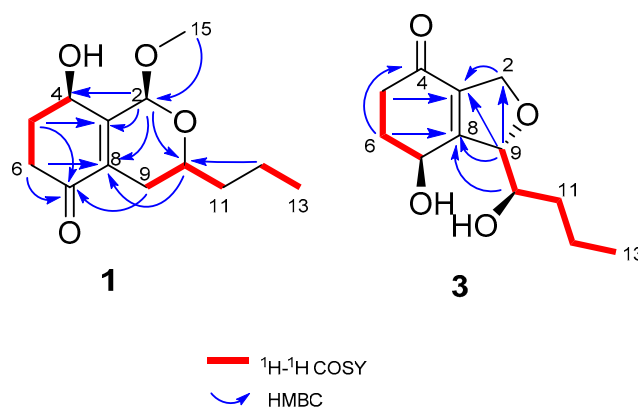
Figure 2. ^{1}H-^{1}H COSY and key HMBC correlations of **1** and **3**.

Two fragments of -CH$_2$(12)-CH$_3$(13) and -CH$_2$(11)-CHO(10)-CH$_2$(9)-, derived from ^{1}H-^{1}H COSY correlations of H$_3$-13 (δ_H 0.95)/H$_2$-12 (δ_H 1.43, 1.52) and H$_2$-9 (δ_H 1.88, 2.36)/H-10 (δ_H 3.74)/H$_2$-11 (δ_H 1.55, 1.61), were connected by the HMBC correlation from H$_2$-12 to C-10 (δ_C 66.7) as one aliphatic chain. Then, this aliphatic chain of -CH$_2$ (9)-CHO (10)-CH$_2$ (11)-CH$_2$ (12)-CH$_3$ (13) was positioned at C-8 according to the HMBC correlations from H-9 to C-7 and H-10 to C-8. C-2 was connected with C-3 (δ_C 151.4) because of the HMBC correlations from H-2 to C-8, C-3, and C-4 (δ_C 65.3), and the oxygen bridge between C-2 and C-10 was determined by the HMBC correlation from H-2 to C-10. The methoxy was positioned at C-2 by the HMBC correlation from H$_3$-15 (δ_H 3.50) to C-2 (δ_C 95.2).

Compound **1** was determined to be a 5,6-deoxy and 2-methoxyated derivative of EI-1941-1 [8] and named phomopsiketone D.

In order to establish the relative configuration of **1**, the Nuclear Overhauser Effect Spectroscopy (NOESY) was measured (Figure S15). NOESY correlations between H-2/H-10 and H-6a/H-4 suggest that both of the cyclohexanone and dihydropyran (DHP) rings were in the twist chair conformation. The cross peaks between H-4/H-2/H-10 suggested that they adopted the same orientations. The absolute configuration of **1** was established by a comparison between the experimental ECD spectrum and the theoretically calculated values of two possible stereoisomers (2*R*, 4*S*, 10*R*)-**1** and (2*S*, 4*R*, 10*S*)-**1** [9,10]. The experimental ECD (Figure 3) of **1** showed a positive Cotton effect at 325 nm and a negative Cotton effect at 230 nm, which matched well with the calculated value of (2*R*, 4*S*, 10*R*)-**1**, and contributed to determining the absolute configuration of **1** as (2*R*, 4*S*, 10*R*).
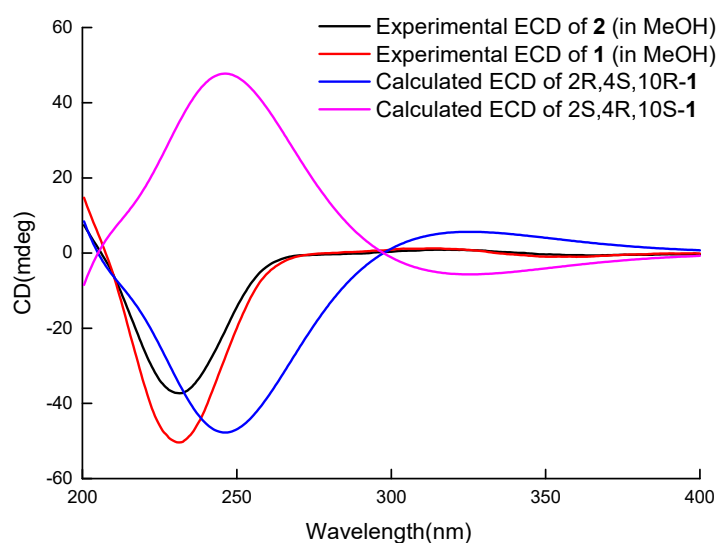

Figure 3. Comparison between calculated ECD spectra of **1** and experimental curves of **1**–**2**.

Compound **2** was obtained as a light brown oil. Its molecular formula was determined to be $C_{18}H_{30}O_5$ (with 4 degrees of unsaturation) on the basis of its HRESIMS (*m/z* 349.1989 for [M+Na]$^+$) and NMR data. IR absorption at 3426 and 1678 cm^{-1} indicated the presence of a hydroxyl and unsaturated ketones. Its ^{13}C NMR and DEPT spectra (Table 2) showed distinctive signals, including one *α*, *β*-unsaturated ketone (δ_C 197.9), two olefinic carbons (δ_C 131.5, 154.4), one ketal carbon (δ_C 95.6), and one oxygenated methine (δ_C 67.4), similar to those of **1**, and indicated that compound **2** contained a similar bicyclic skeleton to that of **1**. Additional signals, including three oxygenated methylenes (δ_C 68.4, 69.9, 71.5), two methylenes (δ_C 31.5, 19.3), and one methyl (δ_C 14.0), were observed, while the methoxy in **1** was absent in **2**. These additional signals were organized as one 2-butoxyethoxy group (CH$_3$(21)-CH$_2$(20)-CH$_2$(19)-CH$_2$(18)-O-CH$_2$(16)-CH$_2$(15)) by ^{1}H-^{1}H COSY correlations of H$_2$-15 (δ_H 3.86, 3.97)/H$_2$-16 (δ_H 3.60, 3.66) and H$_2$-18 (δ_H 3.53)/H$_2$-19 (δ_H 1.61, 1.63)/H$_2$-20 (δ_H 1.36, 1.39)/H$_3$-21 (δ_H 0.94), combined with the HMBC correlations from H$_2$-18 to C-16 and H$_2$-16 to C-18 (Figure S1). The 2-butoxyethoxy group was connected to C-2 through an ether linkage according to the HMBC correlation from H$_2$-15 to C-2 (δ_C 95.6). Thus, compound **2** was elucidated as shown in Figure 1 and named phomopsiketone E.

Table 1. NMR data for compounds **1–7**.

No.	1 [a]	2 [a]	3 [b]	4 [c]	5 [b]	6 [b]	7 [b]
	δ_H (*J* in Hz)	δ_H (*J* in Hz)	δ_H (*J* in Hz)	δ_H (*J* in Hz)	δ_H (*J* in Hz)	δ_H (*J* in Hz)	δ_H (*J* in Hz)
2	5.29, s	5.48, s	4.69, ddd (12.5, 3.1, 2.2) 4.74, ddd (12.0, 5.5, 3.0)	4.76, m 4.97, m	4.02, overlapped 4.30, dt (16.5, 2.3)	4.00, overlapped 4.37, overlapped	4.60, d (15.6) 4.82, d (15.6)
4	4.59, br s	4.63, d (9.2)			4.06, m	3.95, dd (4.5, 5.6)	
5	2.06, m 2.28, m	2.01, m 2.30, m	2.48, m 2.52, m	2.47, m 2.53, dt (16.0, 4.7)	1.54, m 2.02, m	1.74, m 1.79, m	6.63, d (8.0)
6	2.40, m 2.70, ddd (17.0, 7.0, 5.0)	2.40, m 2.65, dt (17.0, 4.0)	2.01, m 2.34, ddd (12.6, 9.4, 4.7)	2.01, m 2.31, ddd (12.8, 9.4, 4.8)	1.56, m 2.07, m	1.72, m 1.82, m	7.07, t (8.0)
7			4.67, m	4.64, m	4.43, m	4.35, overlapped	7.01, d (8.0)
9	1.88, m 2.36, m	1.84, m 2.36, m	5.10, m	4.94, m	3.99, overlapped	3.98, overlapped	4.30, d (8.5)
10	3.74, m	3.70, m	3.80, dt (8.0, 4.0)	3.83, dt (9.5, 3.2)	3.33, overlapped	3.30, overlapped	3.37, m
11	1.55, m 1.61, m	1.54, m 1.59, m	1.52, m 1.54, m	1.39, m 1.44, m	1.46, m 1.75, m	1.48, m 1.72, m	1.50, m 1.89, m
12	1.43, m 1.52, m	1.43, m 1.50, m	1.58, m 1.42, m	1.53, m 1.33, m	1.41, m 1.59, m	1.40, m 1.56, m	1.48, m 1.65, m
13	0.95, t (7.0)	0.94, t (7.0)	0.96, t (7.0)	0.96, t (7.0)	0.96, t (7.2)	0.96, t (7.3)	0.99, t (7.2)
15	3.50, s	3.86, ddd (12.1, 8.8, 2.8) 3.97, dt (12.0, 3.0)					
16		3.60, dt (11.0, 3.0) 3.66, m					
18		3.53, m 3.53, m					
19		1.61, m 1.63, m					
20		1.36, m 1.39, m					
21		0.94, t (7.0)					

[a] Measured in CDCl₃ and at 500 MHz NMR. [b] Measured in CD₃OD and at 500 MHz NMR. [c] Measured in CD₃OD and at 600 MHz NMR.

Table 2. ^{13}C NMR data for compounds **1–7**.

No.	1 [a]	2 [a]	3 [b]	4 [c]	5 [b]	6 [b]	7 [b]
	δ_C, Type	δ_C, Type	δ_C, Type	δ_C, Type	δ_C, Type	δ_C, Type	δ_C, Type
2	95.2, CH	95.6, CH	73.8, CH$_2$	76.0, CH$_2$	67.1, CH$_2$	65.6, CH$_2$	65.3, CH$_2$
3	151.4, C	154.4, C	136.0, C	134.6, C	137.1, C	137.0, C	123.3, C
4	65.3, CH	66.5, CH	197.1, C	197.1, C	67.2, CH	66.1, CH	153.5, C
5	31.3, CH$_2$	30.9, CH$_2$	37.1, CH$_2$	37.6, CH$_2$	29.6, CH$_2$	29.1, CH$_2$	113.8, CH
6	34.4, CH$_2$	36.1, CH$_2$	34.5, CH$_2$	34.1, CH$_2$	29.8, CH$_2$	29.2, CH$_2$	128.3, CH
7	198.2, C	197.9, C	66.0, CH	65.7, CH	64.2, CH	64.4, CH	118.9, CH
8	132.5, C	131.5, C	163.6, C	167.0, C	135.5, C	135.3, C	140.0, C
9	27.4, CH$_2$	27.2, CH$_2$	91.3, CH	90.0, CH	67.0, CH	67.0, CH	70.1, CH
10	66.7, CH	67.4, CH	74.4, CH	74.0, CH	80.4, CH	80.2, CH	80.4, CH
11	37.4, CH$_2$	37.2, CH$_2$	35.6, CH$_2$	34.1, CH$_2$	35.2, CH$_2$	35.0, CH$_2$	35.5, CH$_2$
12	18.9, CH$_2$	18.8, CH$_2$	20.0, CH$_2$	20.1, CH$_2$	20.0, CH$_2$	19.9, CH$_2$	19.8, CH$_2$
13	14.1, CH$_3$	14.0, CH$_3$	14.4, CH$_3$	14.4, CH$_3$	14.4, CH$_3$	14.4, CH$_3$	14.4, CH$_3$
15	55.8, CH$_3$	68.4, CH$_2$					
16		69.9, CH$_2$					
18		71.5, CH$_2$					
19		31.5, CH$_2$					
20		19.3, CH$_2$					
21		14.0, CH$_3$					

[a] Measured in CDCl$_3$ and at 125 MHz NMR. [b] Measured in CD$_3$OD and at 125 MHz NMR. [c] Measured in CD$_3$OD and at 150 MHz NMR.

The DHP and cyclohexanone rings were also in twist chair conformations according to the NOESY correlation between H-2 and H-10 as well as the H-6 axial and H-4. The ECD spectra (Figure 3) of **1** and **2** showed similar curves (the cotton effect was positive at 325 nm (**1**) and 325 nm (**2**), and negative at 230 nm (**1**) and 228 nm (**2**)), and determined the absolute configurations of (2*R*, 4*S*, 10*R*) for **2**.

Compound **3** was obtained as a yellow oil. Its molecular formula was determined to be C$_{12}$H$_{18}$O$_4$ (with 4 degrees of unsaturation) on the basis of its HRESIMS (*m/z* 261.0895 for [M+Cl]$^-$) and NMR data. Carbon NMR (Table 2) showed 12 signals, including one *α*, *β*-unsaturated ketone (δ_C 197.1), two olefinic carbons (δ_C 136.0, 163.6), nine aliphatic carbons that were grouped into one methyl (δ_C 14.4), five methylenes (δ_C 20.0, 34.5, 35.6, 37.1, and 73.8 (oxygenated)), and three oxygenated methines (δ_C 66.0, 74.4, 91.3), by an Heteronuclear singular Quantum Coherence (HSQC) spectrum. These signals were similar to those of phomopsiketone A [11] except that one methylene in **3** replaced one oxygenated methine in phomopsiketone A. Several NMR signals, including a multiplet for H-7 (δ_H 4.67) (Table 1), and ^{1}H-^{1}H COSY correlations of H-7/H$_2$-6/H$_2$-5 (Figure 2) indicated the presence of 6-CH$_2$. Thus, **3** was determined to be 6-deoxy-phomopsiketone A and named phomopsiketone F.

The absolute configuration of **3** was determined by a modified version of Mosher's esterification method [12,13]. Compound **3** was acylated with R-(−)-and S-(+)-*α*-methoxy-*α* (trifluoromethyl) phenylacetyl chloride (*α*-MTPA-Cl). The products were separated by preparative HPLC and purified as six compounds, which were determined to be the 7-*S*-MTPA ester (**3a**), 7-*R*-MTPA ester (**3b**), 10-*S*-MTPA ester (**3c**), 10-*R*-MTPA ester (**3d**), 7,10-*di*-*S*-MTPA ester (**3e**), and 7,10-*di*-*R*-MTPA ester (**3f**) by HRESIMS (7,10-*S*-MTPA ester, *m/z* 465.1500; 7,10-*R*-MTPA ester, *m/z* 465.1497; 7,10-*di*-*S*-MTPA ester, *m/z* 681.1896; 7,10-*di*-*R*-MTPA ester, *m/z* 681.1893 for [M+Na]$^+$, Figures S86, S87, S89, S90, S93 and S94, respectively), ^{1}H NMR data (δ_{H-7} 6.14 for **3a**, 6.13 for **3b**; δ_{H-10} 5.40 for **3c**, 5.42 for **3d**, Figures S84 and S88, respectively), and the ^{1}H-^{1}H COSY correlations (Figure S85) of H-7 (δ_H 6.14)/H-6 (δ_H 2.09, 2.47) and H-10 (δ_H 3.67)/H-11 (δ_H 1.55, 1.44) in **3a**. A comparison of proton chemical shifts between 3a/3b and 3c/3d ($\Delta\delta_{3a-3b}$ and $\Delta\delta_{3c-3d}$, Figure 4) determined the configurations of C-7 and C-10 to be 7*S* and 10*R*, respectively. A NOESY correlation between H-7 (δ_H 5.92) and H-10 (δ_H 5.31) was observed in 3f and allowed us to deduce the configuration of C-9 as *S* (Figures S5 and S92). Thus, the absolute configuration of **3** was determined to be (7*S*, 9*S*, 10*R*).
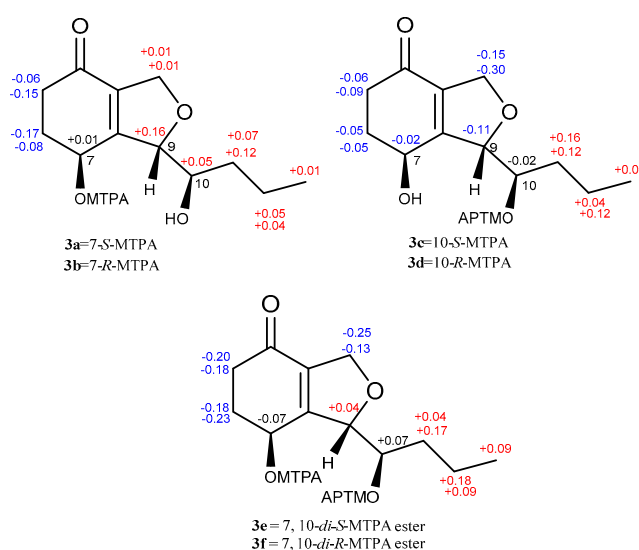
Figure 4. $\Delta\delta_{S\text{-}R}$ values for the MTPA esters (**3a/3b**, **3c/3d**, and **3e/3f**).

Compound **4** was also obtained as a yellow oil. Its molecular formula was established as $C_{12}H_{18}O_4$, identical to that of **3**, by HRESIMS (*m/z* 249.1101 for [M+Na]$^+$) and NMR data. The proton and carbon spectra were also similar to those of **3** (Tables 1 and 2) and a two-dimensional (2D) NMR analysis (Figure S2) enabled us to deduce that it has the same planar structure as **3**. Different ECD spectra of **3** and **4** (Figure S8) were used to confirm that they were stereoisomers.

A NOESY correlation between H-7 and H-9 was not observed. Then, the modified version of Mosher's esterification method was applied to determine the absolute configuration of **4**. Esterification of **4** with (*R*)- and (*S*)-MTPA-Cl yielded the 7,10-*di*-*S*-MTPA ester (**4a**) and the 7,10-*di*-*R*-MTPA ester (**4b**), respectively. The similar ^{1}H NMR chemical shift differences ($\Delta\delta_{\mathbf{4e\text{-}4f}}$, Figure S6 and Figure 3) around the C-7 and C-10 stereocenters as **3** indicated the 7*S* and 10*R* configurations for **4**. Since **4** was the stereoisomer of **3,** the configuration of C-9 in **4** was deduced to be *R*, contrary to that in **3**. Thus, the absolute configuration of **4** was determined to be (7*S*, 9*R*, 10*R*) and it was named phomopsiketone G.

Compound **5** was crystallized as colorless needles in acetone. Its HRESIMS showed an ion peak [M+Na]$^+$ at *m/z* 251.1258, corresponding to the molecular formula $C_{12}H_{20}O_4$ and possessing two hydrogen atoms more than **3** and **4**. A comparison of ^{13}C NMR data between **3** and **5** revealed that the ketone carbonyl (δ_C 197.1, C-4 in **3**) was replaced by one oxygenated methine (Table 2). ^{1}H-^{1}H COSY correlations between H-4 (δ_H 4.06)/H-5 (δ_H 1.54, 2.02)/H-6 (δ_H 1.56, 2.07)/ H-7(δ_H 4.43) (Figure S3) confirmed that the ketone carbonyl was hydrogenated. A similar C_5 side chain (CH_3-13/CH_2-12/CH_2-11/CH-10/CH-9) to that in **3** was derived from ^{1}H-^{1}H COSY correlations (Figure S3). Key HMBC correlations from H-2 (δ_H 4.02) to C-10 (δ_C 80.4) and H-9 (δ_H 3.99) to C-3 (δ_C 137.1) (Figure S3) indicated the presence of a dihydropyran fragment that was different from the dihydrofuran in **3**. Thus, **5** was determined to be a new polyketide and named letendronol A.

In order to establish the relative configuration, **5** was crystallized and, by use of X-ray analysis (Figure 5), H-4 and H-9 were assigned to the same orientation, and H-7 and H-10 were assigned to the opposite orientation of H-4 and H-9.

The *tri*-(*S/R*) MTPA esters (**5a/5b**) were obtained by the modified version of Mosher's method together with HPLC purification. A ^{1}H NMR data comparison of **5a** and **5b** ($\Delta\delta_{\mathbf{5a\text{-}5b}}$, Figure S7) determined the absolute configurations of (4*S*, 7*S*, 9*R*) in **5**. Finally, the configuration of **5** was unambiguously confirmed to be (4*S*, 7*S*, 9*R*, and 10*S*) by X-ray analysis combined with the modified version of Mosher's method.

Compound **6** was contained as a colorless amorphous powder. It has the same molecular formula ($C_{12}H_{20}O_4$) as **5** according to its HRESIMS (*m/z* 251.1260 for [M+Na]$^+$) and ^{13}C NMR data. One dimensional (1D) NMR data (Tables 1 and 2) combined with a 2D NMR analysis (Figure S3) revealed **6**

to have the same planar structure as **5**. Compound **6** was deduced to be a stereoisomer of **5** because of their different retention times when eluted by the same HPLC program and was named letendronol B.
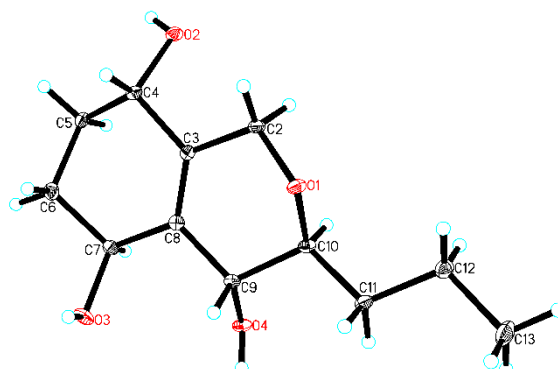

Figure 5. The X-ray crystal structure of **5** (the thermal ellipsoid was 30%).

Compounds **6** and **5** contained different a configuration at C-4, which was assigned by the modified version of Mosher's method. Treatment of **6** with (*R*)- or (*S*)-MTPA-Cl yielded the *tri*-(*S*/*R*) MTPA esters (**6a**/**6b**). The result of the application of the modified version of Mosher's method ($\Delta\delta_{\text{6a-6b}}$, Figure S7) revealed 7*S* and 9*R* configurations, identical to **5**, and a 4*R* configuration different from **5**, in **6**. H-9 and H-10 were also assigned to different orientations according to the broad singlet peaks for H-9 in **6a** (δ_H 5.11, br s) and **6b** (δ_H 4.78, br s) (Figure S110), similar to those in **5a** (δ_H 5.19, br s) and **5b** (δ_H 4.76, br s) (Figure S98). Then, the absolute configuration of **6** was determined to be (4*R*, 7*S*, 9*R*, and 10*S*).

Compound **7** was obtained as a white amorphous powder. The molecular formula of **7** was determined to be $C_{12}H_{16}O_3$ with 5 degrees of unsaturation by its HRESIMS (*m/z* 231.0995 for [M+Na]$^+$) and NMR data. The ^{1}H NMR (Table 1) of **7** displayed one methyl (δ_H 0.99, 3H, t, *J* = 7.2 Hz) and three aromatic protons (δ_H 6.63, 1H, d, *J* = 8.0 Hz; δ_H 7.07, 1H, t, *J* = 8.0 Hz; δ_H 7.01, 1H, d, *J* = 8.0 Hz) whose coupling constants revealed their *ortho*-relationship. The ^{13}C NMR spectrum (Table 2) showed 12 signals, which were assigned by HSQC data to six aromatic carbons (δ_C 153.5, 113.8, 128.3, 118.9, 140.0, and 123.3), two oxygenated methines (δ_C 80.4, 70.1), one oxygenated methylene (δ_C 65.3), two methylenes (δ_C 35.5 and 19.8), and one methyl carbon (δ_C 14.4). A similar C_5 side chain to those in **3–6** was derived from ^{1}H-^{1}H COSY correlations (Figure S4) between H-13 (δ_H 0.99)/H$_2$-12 (δ_H 1.48, 1.65)/H$_2$-11 (δ_H 1.50, 1.89)/H-10 (δ_H 3.37)/H-9 (δ_H 4.30) and connected with the aromatic ring at C-8 (δ_C 140.0) according to the HMBC correlations from H-9 to C-8 (δ_C 140.0), C-3 (δ_C 123.3), and C-7 (δ_C 118.9). Meanwhile, oxygenated CH$_2$ (δ_C 65.3, C-2) was connected with C-3 (δ_C 123.3) because of the HMBC correlations from H$_2$-2 (δ_H 4.60, 4.82) to C-3, C-8, and C-4 (δ_C 153.5). The oxygen bridge between C-2 and C-10 (δ_C 80.4) was determined by the HMBC correlation from H-2 to C-10. Thus, compound **7** was determined to be a new polyketide containing an isochroman skeleton and named letendronol C. The vicinal coupling constant $J_{\text{H-9/H-10}}$ (8.5 Hz) indicated a *trans* relationship between H-9 and H-10. A comparison of the optical rotation of **7** ($[\alpha]^{20}_D$ +9) with that of (3*R*,4*S*)-6,8-Dihydroxy-1,1-dimethyl-3,4,5-trimethylisochroman [14] ($[\alpha]^{25}_D$ -28.5) was used to determine that the absolute configurations at C-9 and C-10 were *R* and *S*, respectively. The 9*R* and 10*S* configurations of **7** were also confirmed by a comparison between the experimental ECD spectrum and the theoretically calculated values of (9*R*, 10*S*)-**7**. The experimental ECD (Figure 6) of **7** showed a positive Cotton effect at 195 and a negative Cotton effect at 205 nm, which matched well with the calculated value of (9*R*, 10*S*)-**7**.
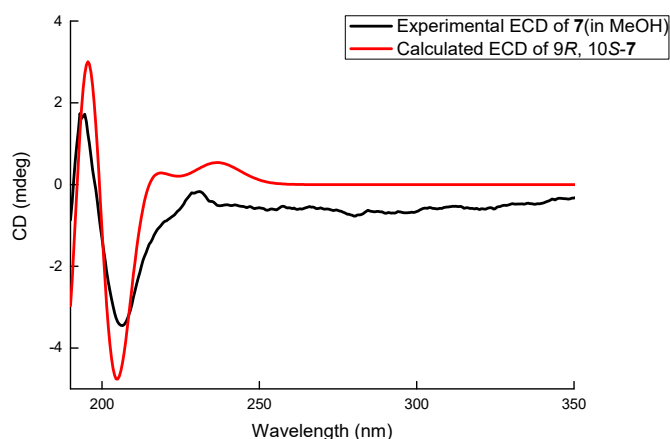
Figure 6. The comparison between calculated ECD spectra and the experimental curve of **7**.

The known compound **8** was determined to be xylarinol by comparison of its NMR data with the reported literature [15].

Compounds **1**, **2**, **3**, and **5** were evaluated for their inhibitory activities against Lipopolysaccharide (LPS)-activated NO production in RAW264.7 [16], and all tested compounds showed no cytotoxicity to macrophage cells at the concentration of 100 μM and 50 μM by the MTT method. Compound **2** showed weak anti-inflammatory activity with an IC_{50} value of 86 μM. Hydrocortisone was used as a positive control with the IC_{50} value of 22.4 μM. The other compounds showed no anti-inflammatory activity with IC_{50} values of >100 μM. All compounds were assayed for their cytotoxicity against the prostate cancer PC3 cell line by the MTT method [17]. Compounds **1**–**3**, **5**, **6**, and **8** were also assayed for antibacterial activity against *Staphylococcus aureus*, *Staphylococcus epidermidis*, *Escherichia coli*, *Miconia albicans* and *Pseudomonas aeruginosa* using the Kirby−Bauer Diffusion method. Regrettably, none of these compounds showed any activities in the cytotoxicity and antibacterial tests.

3. Materials and Methods

3.1. General Experimental Procedures

Optical rotations were measured on Rudolph research analytical AUTOPOL I. The ultraviolet spectra were obtained from a Shimadzu UV-1800 spectrophotometer using MeOH as the solvent. Electronic circular dichroism (ECD) spectra were obtained on a JASCO J-1500 circular dichroism. The infrared (IR) spectra were acquired from a Bruker Vector 22. NMR spectra were recorded on a Bruker AVIII 500 MHz and JEOL 600 Hz, using TMS as the internal standard. HRESIMS spectra were obtained from an Agilent 6224 TOF LC/MS. Analytical HPLC was performed on an Agilent 1260 system using a C18 (Cosmosil, 5 μm, 4.6 × 250 mm) column. The column chromatography was carried out using Silica gel (200–300 mesh, Qing Dao Hai Yang Chemical Group Co., Qing Dao, China).

3.2. Fungal Material and Fermentation

The *Letendraea* sp. was isolated from the gut of a crab found on Zhairuoshan Island (N20.2920, E122.5), Zhoushan, Zhejiang Province, China, in August 2015. The fungus was determined to be *Letendraea* sp. by 26s rDNA sequence analysis (GenBank accession no. MK743951), and produced a sporulating, white-colored culture when growing on potato-dextrose agar (PDA). The strain was deposited (NO. 5XNZ4-2) at the Institute of Marine Biology of Zhejiang University. The strain was static cultured at 28 °C for 30 days in 500 mL Erlenmeyer flasks (100 × 200 mL, a total of 20 L) each containing 200 mL of 1/2 PDB liquid media (100 g of potato extract, 17 g of artificial sea salt, and 10 g of dextrose in 1 L pure water).

3.3. Extraction and Isolation

The culture broth (20 L) was filtered and extracted with equivoluminal EtOAc three times to obtain 2.79 g of metabolite extract, which was fractionated by column chromatography (CC) over silica gel (200−300 mesh, 60 g) and eluted in a gradient of petroleum ether (P)-EtOAc(E) (20:1–1:1) to yield 10 fractions (Frs. 1–10) based on TLC analysis. Fr. 7 was further separated via preparative HPLC with a C18 (Agilent, 10 μm, 21.2 × 250 mm) column at 210 nm, eluting with MeOH/H_2O (40/60, v/v) at 8 mL/min to obtain four sub-fractions (Fr. 7.1–7.4). Fr. 7.1 (110 mg) was purified with semi-preparative HPLC (Agilent C18 column, 10 μm, 10 × 250 mm, MeCN/H_2O 10:90, 4 mL/min, 210 nm) to yield **3** (73 mg). Fr. 10 was purified by CC over silica gel (200−300 mesh, 30 g) using a gradient of CH_2Cl_2-MeOH (50:1–1:1) as a mobile phase to provide five fractions (Fr. 11–15). Fr. 13 was also separated via preparative HPLC (Agilent C18 column, 10 μm, 21.2 × 250 mm, 210 nm), eluting with MeOH/H_2O (15/85, v/v) at 10 mL/min to obtain **5** (148 mg) and other three sub-fractions (Fr. 13.1–13.3). Fr. 13.2 (64 mg) was further purified on semi-preparative HPLC (Agilent C18 column, 10 μm, 10 × 250 mm, MeOH/H_2O 15:85, 4 mL/min, 210 nm) to yield **6** (14 mg). Fr. 8 was initially separated by CC over silica gel (200−300 mesh, 60 g) with a dichloromethane (D) and MeOH (M) gradient from 80:1 to 5:1 based on TLC analysis to afford 10 sub-fractions (Fr. 8.1–8.10). Sub-fractions Fr. 8.3 (142 mg), Fr. 8.5 (33 mg), Fr. 8.9 (24.2 mg), and Fr. 8.10 (45.7 mg) were all further purified by semi-preparative HPLC (Agilent C18 column, 10 μm, 10 × 250 mm, 230 nm) at 4 mL/min using MeCN/H_2O (63/37, v/v), MeCN/H_2O (25/75, v/v), MeOH/H_2O (18/82, v/v), and MeOH/H_2O (35/65, v/v) as the eluting solvents, respectively. Compounds **1** (16.4 mg) and **2** (19.2 mg) were acquired from Fr. 8.3. Compounds **7** (7.7 mg), **4** (2.7 mg), and **8** (19.4 mg) were obtained from Fr. 8.5, Fr. 8.9, and Fr. 8.10, respectively.

Phomopsiketone D (**1**): Yellow amorphous powder; molecular formula $C_{13}H_{20}O_4$; [α] ^{20} $_D$ −60 (c 0.1, MeOH); ECD (0.50 mg/mL, MeOH) λmax (Δ ε) 350 (−0.97), 311 (+1.24), 230 (−50.40), 194 (+27.24) nm; UV (MeOH) λmax (log ε) 232 (3.93) nm; IR (λmax) 3426, 2957, 2933, 2874, 2830, 1672, 1422, 1380, 1332, 1280, 1189, 1172, 1095, 1066, 1040, 979, 950, 906 cm^{-1}; ^{1}H NMR data (500 MHz, in CDCl$_3$) and ^{13}C NMR data (125 MHz, in CDCl$_3$), see Tables 1 and 2; HRESIMS *m/z* [M+Na]$^+$ 263.1256 (calcd. for $C_{13}H_{20}O_4Na$, 263.1259).

Phomopsiketone E (**2**): Light brown oil; molecular formula $C_{18}H_{30}O_5$; [α] ^{20} $_D$ −60 (c 0.1, MeOH); ECD (0.50 mg/mL, MeOH) λmax (Δ ε) 365 (−0.64), 311 (+0.87), 230 (−37.30), 194 (+15.31) nm; UV (MeOH) λmax (log ε) 232 (3.99) nm; IR (λmax) 3437, 2958, 2932, 2873, 1678, 1462, 1326, 1279, 1172, 1121, 1074, 1034, 924, 906 cm^{-1}; ^{1}H NMR data (500 MHz, in CDCl$_3$) and ^{13}C NMR data (125 MHz, in CDCl$_3$), see Tables 1 and 2; HRESIMS *m/z* [M+Na]$^+$ 349.1989 (calcd. for $C_{18}H_{30}O_5Na$, 349.1991).

Phomopsiketone F (**3**): Yellow oil; molecular formula $C_{12}H_{18}O_4$; [α] ^{20} $_D$ −30 (c 0.1, MeOH); ECD (0.40 mg/mL, MeOH) λmax (Δ ε) 323 (+9.56), 259 (−48.72), 203 (+58.04) nm; UV (MeOH) λmax (log ε) 257 (3.75), 210 (3.80) nm; IR (λmax) 3437, 2961, 2870, 1671, 1542, 1398, 1124, 1071, 1026, 922, 849 cm^{-1}; ^{1}H NMR data (500 MHz, in CD$_3$OD) and ^{13}C NMR data (125 MHz, in CD$_3$OD), see Tables 1 and 2; HRESIMS *m/z* [M+Cl]$^-$ 261.0895 (calcd. for $C_{12}H_{18}O_4Cl$, 261.0894).

Phomopsiketone G (**4**): Yellow oil; molecular formula $C_{12}H_{18}O_4$; [α] ^{20} $_D$ −2 (c 0.1, MeOH); ECD (0.45 mg/mL, MeOH) λmax (Δ ε) 322 (−2.76), 255 (−12.86), 204 (+34.78) nm; UV (MeOH) λmax (log ε) 225 (4.18) nm; IR (λmax) 3386, 2958, 2932, 2872, 1665, 1460, 1395, 1125, 1074, 1003, 947, 855 cm^{-1}; ^{1}H NMR data (600 MHz, in CD$_3$OD) and ^{13}C NMR data (150 MHz, in CD$_3$OD), see Tables 1 and 2; HRESIMS *m/z* [M+Na]$^+$ 249.1101 (calcd. for $C_{12}H_{18}O_4Na$, 249.1103).

Letendronol A (**5**): Colorless needle-like crystal from acetone; mp 159–160 °C; molecular formula $C_{12}H_{20}O_4$; [α] ^{20} $_D$ −5 (c 0.1, MeOH); ECD (0.50 mg/mL, MeOH) λmax (Δ ε) 213 (−60.56), 194 (+41.96) nm; UV (MeOH) λmax (log ε) 263 (2.37) nm; IR (λmax) 3338, 3295, 2953, 2921, 2866, 1459, 1322, 1292, 1155, 1120, 1070, 1034, 1005, 924, 905 cm^{-1}; ^{1}H NMR data (500 MHz, in CD$_3$OD) and ^{13}C NMR data (125 MHz, in CD$_3$OD), see Tables 1 and 2; HRESIMS *m/z* [M+Na]$^+$ 251.1258 (calcd. for $C_{12}H_{20}O_4Na$, 251.1259).

Letendronol B (**6**): Colorless amorphous powder; molecular formula $C_{12}H_{20}O_4$; $[\alpha]^{20}$ D –3 (c 0.1, MeOH); ECD (0.40 mg/mL, MeOH) λmax (Δ ε) 214 (–20.71), 195 (+31.03) nm; UV (MeOH) λmax (log ε) 263 (2.37) nm; IR (λmax) 3354, 2956, 2872, 1447, 1332, 1280, 1186, 1152, 1102, 1054, 1005, 970, 948 cm^{-1}; ^{1}H NMR data (500 MHz, in CD$_3$OD) and ^{13}C NMR data (125 MHz, in CD$_3$OD), see Tables 1 and 2; HRESIMS *m/z* [M+Na]$^+$ 251.1260 (calcd. for $C_{12}H_{20}O_4Na$, 251.1259).

Letendronol C (**7**): White amorphous powder; molecular formula $C_{12}H_{16}O_3$; $[\alpha]^{20}$ D +9 (c 0.1, MeOH); ECD (0.40 mg/mL, MeOH) λmax (Δ ε) 280 (–0.77), 206 (–3.45) nm; UV (MeOH) λmax (log ε) 275 (3.03), 205 (3.96) nm; IR (λmax) 3354, 2958, 2930, 2872, 1593, 1469, 1366, 1280, 1230, 1090, 1049, 1015, 964, 898, 840, 803, 762 cm^{-1}; ^{1}H NMR data (500 MHz, in CD$_3$OD) and ^{13}C NMR data (125 MHz, in CD$_3$OD), see Tables 1 and 2; HRESIMS *m/z* [M+Na]$^+$ 231.0995 (calcd. for $C_{12}H_{16}O_3Na$, 231.0997).

3.4. ECD Calculation of Compound 1

Monte Carlo conformational searches were carried out by means of the Spartan's 10 software using Merck Molecular Force Field (MMFF). The conformers with a Boltzmann population of over 5% were chosen for ECD calculations, and then the conformers were initially optimized at the B3LYP/6-31+g (d, p) level in MeOH using the CPCM polarizable conductor calculation model. The theoretical calculation of ECD was conducted in MeOH using time-dependent density functional theory (TD-DFT) at the B3LYP/6-311+g (d, p) level for all conformers of compound **1**. Rotatory strengths for a total of 50 excited states were calculated. ECD spectra were generated using the program SpecDis 1.6 (University of Würzburg, Würzburg, Germany) and GraphPad Prism 5 (University of California San Diego, USA) from dipole-length rotational strengths by applying Gaussian band shapes with sigma = 0.3 eV [18].

3.5. Preparation of MTPA Esters of Compound 3

Compound **3** (4 mg, 8.85 μmol each) in 1 mL of anhydrous pyridine was separated into two equal portions. (*R*)- or (*S*)-MTPA chloride (5 μL, 26.6 μmol each) was added into the two portions, respectively. Each reaction mixture was stirred at ambient temperature for 4 h and the reaction was terminated by adding 1 mL of methanol. The reaction mixtures were dried under vacuum and separated by HPLC (column: Agilent ODS column, 10.0 × 250 mm; mobile phase: MeOH-H$_2$O, 70:30 (v/v); flow rate: 4 mL/min) to afford the 7-*S*-MTPA ester (**3a**, 0.56 mg), 7-*R*-MTPA ester (**3b**, 0.68 mg), 10-*S*-MTPA ester (**3c**, 1.02 mg), 10-*R*-MTPA ester (**3d**, 0.96 mg), 7,10-*di*-*S*-MTPA ester (**3e**, 0.73 mg), and 7,10-*di*-*R*-MTPA ester (**3f**, 0.85 mg) of **3**.

3.6. Preparation of MTPA Esters of Compounds 4–6

Compounds **4** (1 mg), **5** (4 mg), and **6** (1.5 mg) in 1 mL of anhydrous pyridine were separated into two equal portions. (*R*)- or (*S*)-MTPA chloride (50 μL each) was added into each portion, respectively. Each reaction mixture was stirred at ambient temperature for 4 h and the reaction was terminated by adding 1 mL of methanol. HPLC was also used for the isolation of (*S*)-MTPA ester -**4** (**4a**, 0.7 mg) and (*R*)-MTPA ester -**4** (**4b**, 0.7 mg). The (*S*)-MTPA and (*R*)-MTPA esters of **5** (**5a**, 5.0 mg; **5b**, 5.7 mg) and **6** (**6a**, 2.30 mg; **6b**, 1.92 mg) were also prepared in a similar manner.

7-*S*-MTPA Ester of **3** (**3a**): White amorphous solid. ^{1}H NMR (600 MHz, in CD$_3$OD) δ$_H$ 7.30−7.64 (5H, m, MTPA-Ar), 6.14 (1H, brs, H-7), 4.81 (1H, m, H-9), 4.73 (1H, ddd, *J* = 13.0, 6.0, 2.6 Hz, H-2a), 4.68 (1H, ddd, *J* = 13.0, 6.0, 1.6 Hz, H-2b), 3.67 (1H, m, H-10), 3.57 (3H, brs, MTPA-OMe), 2.51 (1H, m, H-5a), 2.47 (1H, m, H-6a), 2.38 (1H, m, H-5b), 2.09 (1H, m, H-6b), 1.58 (1H, m, H-12a), 1.55 (1H, m, H-11a), 1.44 (1H, m, H-11b), 1.39 (1H, m, H-12b), 0.94 (3H, t, *J* = 7.0 Hz, H-13); HRESIMS *m/z* [M+Na]$^+$ 465.1500 (calcd. for $C_{22}H_{25}F_3O_6Na$, 465.1501).

7-*R*-MTPA Ester of **3** (**3b**): White amorphous solid. ^{1}H NMR (600 MHz, in CD$_3$OD) δ$_H$ 7.32−7.64 (5H, m, MTPA-Ar), 6.13 (1H, brs, H-7), 4.72 (1H, ddd, *J* = 12.8, 6.0, 2.7 Hz, H-2a), 4.67 (1H, m, H-2b) 4.65 (1H, m, H-9), 3.62 (1H, m, H-10), 3.56 (3H, brs, MTPA-OMe), 2.57 (1H, m, H-5a), 2.55 (1H, m, H-6a), 2.53 (1H, m, H-5b), 2.26 (1H, m, H-6b), 1.54 (1H, m, H-12a), 1.43 (1H, m, H-11a), 1.37 (1H, m,

H-11b), 1.34 (1H, m, H-12b), 0.93 (3H, t, *J* = 7.3 Hz, H-13); HRESIMS *m/z* [M+Na]$^+$ 465.1497 (calcd. for C$_{22}$H$_{25}$F$_3$O$_6$Na, 465.1501).

10-*S*-MTPA Ester of **3** (**3c**): White amorphous solid. ^{1}H NMR (600 MHz, in CD$_3$OD) δ_H 7.30−7.64 (5H, m, MTPA-Ar), 5.40 (1H, ddd, *J* = 8.3, 5.6, 1.8 Hz, H-10), 5.30 (1H, m, H-9), 4.52 (1H, m, H-2a), 4.50 (1H, m, H-7), 4.35 (1H, ddd, *J* = 13.0, 5.7, 3.0 Hz, H-2b), 3.55 (3H, m, MTPA-OMe), 2.43 (1H, m, H-5a), 2.27 (1H, m, H-5b), 2.24 (1H, m, H-6a), 1.94 (1H, m, H-6b), 1.84 (1H, m, H-12a), 1.78 (1H, m, H-11a), 1.47 (1H, m, H-11b), 1.43 (1H, m, H-12b), 0.98 (3H, t, *J* = 7.4 Hz, H-13); HRESIMS *m/z* [M+Na]$^+$ 465.1500 (calcd. for C$_{22}$H$_{25}$F$_3$O$_6$Na, 465.1501).

10-*R*-MTPA Ester of **3** (**3d**): White amorphous solid. ^{1}H NMR (600 MHz, in CD$_3$OD) δ_H 7.31−7.64 (5H, m, MTPA-Ar), 5.42 (1H, m, H-10), 5.41 (1H, m, H-9), 4.67 (1H, m, H-2a), 4.65 (1H, m, H-2b), 4.52 (1H, m, H-7), 3.54 (3H, d, *J*=1.0 Hz, MTPA-OMe), 2.49 (1H, m, H-5a), 2.36 (1H, m, H-5b), 2.29 (1H, m, H-6a), 1.99 (1H, m, H-6b), 1.80 (1H, m, H-12a), 1.62 (1H, m, H-11a), 1.35 (1H, m, H-11b), 1.31 (1H, m, H-12b), 0.92 (3H, t, *J* = 7.4 Hz, H-13); HRESIMS *m/z* [M+Na]$^+$ 465.1497 (calcd. for C$_{22}$H$_{25}$F$_3$O$_6$Na, 465.1501).

7, 10-*di-S*-MTPA Ester of **3** (**3e**): White amorphous solid. ^{1}H NMR (600 MHz, in CD$_3$OD) δ_H 7.39−7.52 (10H, m, MTPA-Ar), 5.85 (1H, m, H-7), 5.38 (1H, ddd, *J* = 9.2, 4.8, 1.8 Hz, H-10), 5.11 (1H, ddd, *J* = 6.0, 3.7, 1.8 Hz, H-9), 4.58 (1H, ddd, *J* = 13.3, 3.8, 1.0 Hz, H-2α), 4.45 (1H, ddd, *J* = 13.3, 5.9, 2.1 Hz, H-2β), 3.57 (3H, d, *J* = 1.0 Hz, MTPA-OMe), 3.52 (3H, d, *J* = 1.0 Hz, MTPA-OMe), 2.34 (1H, m, H-5α), 2.30 (1H, m, H-5β), 2.19 (1H, m, H-6α), 2.13 (1H, m, H-6β), 1.78 (1H, m, H-12α), 1.66 (1H, m, H-11α), 1.46 (1H, m, H-11β), 1.41 (1H, m, H-12β), 0.97 (3H, t, *J* = 7.3 Hz, H-13); HRESIMS *m/z* [M+Na]$^+$ 681.1896 (calcd. for C$_{32}$H$_{32}$F$_6$O$_8$Na, 681.1899).

7, 10-*di-R*-MTPA Ester of **3** (**3f**): White amorphous solid. ^{1}H NMR (600 MHz, in CD$_3$OD) δ_H 7.38−7.53 (10H, m, MTPA-Ar), 5.92 (1H, t, *J* = 4.9 Hz, H-7), 5.31 (1H, ddd, *J* = 10.3, 3.8, 2.0 Hz, H-10), 5.08 (1H, td, *J* = 4.8, 2.0 Hz, H-9), 4.71 (1H, m, H-2α), 4.69 (1H, m, H-2β), 3.58 (3H, d, J = 0.8 Hz, MTPA-OMe), 3.52 (3H, d, *J* = 0.8 Hz, MTPA-OMe), 2.54 (1H, m, H-5α), 2.48 (1H, m, H-5β), 2.42 (1H, m, H-6α), 2.31 (1H, m, H-6β), 1.69 (1H, m, H-12α), 1.43 (1H, m, H-11α), 1.29 (1H, m, H-11β), 1.23 (1H, m, H-12β), 0.88 (3H, t, *J* = 7.4 Hz, H-13); HRESIMS *m/z* [M+Na]$^+$ 681.1893 (calcd. for C$_{32}$H$_{32}$F$_6$O$_8$Na, 681.1899).

S-MTPA Ester of **4** (**4a**): White amorphous solid. ^{1}H NMR (600 MHz, in CD$_3$OD) δ_H 7.39−7.48 (10H, m, MTPA-Ar), 5.96 (1H, m, H-7), 5.46 (1H, ddd, *J* = 9.0, 4.6, 1.9 Hz, H-10), 5.16 (1H, m, H-9), 4.72 (1H, *J* = 16.3, 3.6, 1.6 Hz„ H-2a), 4.65 (1H, *J* = 16.3, 5.9, 0.7 Hz„ H-2b), 3.49 (3H, s, MTPA-OMe), 3.38 (3H, s, MTPA-OMe), 2.54 (1H, m, H-5a), 2.49 (1H, m, H-5b), 2.47 (1H, m, H-6a), 2.03 (1H, m, H-6b), 1.70 (1H, m, H-12a), 1.52 (1H, m, H-11a), 1.36 (1H, m, H-11b), 1.30 (1H, m, H-12b), 0.88 (3H, t, *J* = 7.4 Hz, H-13); HRESIMS *m/z* [M+Na]$^+$ 681.1898 (calcd. for C$_{32}$H$_{32}$F$_6$O$_8$Na, 681.1899).

R-MTPA Ester of **4** (**4b**): White amorphous solid. ^{1}H NMR (600 MHz, in CD$_3$OD) δ_H 7.38−7.53 (10H, m, MTPA-Ar), 6.02 (1H, m, H-7), 5.42 (1H, ddd, *J* = 10.3, 3.9, 1.9 Hz, H-10), 5.25 (1H, m, H-9), 4.67 (1H, *J* = 16.3, 3.7, 1.5 Hz„ H-2a), 4.48 (1H, *J* = 16.5, 5.9, 1.0 Hz„ H-2b), 3.54 (3H, brs, MTPA-OMe), 3.50 (3H, brs, MTPA-OMe), 2.59 (1H, m, H-5a), 2.55 (1H, m, H-5b), 2.51 (1H, m, H-6a), 2.20 (1H, m, H-6b), 1.58 (1H, m, H-12a), 1.28 (1H, m, H-11a), 1.16 (1H, m, H-11b), 1.09 (1H, m, H-12b), 0.76 (3H, t, *J* = 7.5 Hz, H-13); HRESIMS *m/z* [M+Na]$^+$ 681.1904 (calcd. for C$_{32}$H$_{32}$F$_6$O$_8$Na, 681.1899).

S-MTPA Ester of **5** (**5a**): White amorphous solid. ^{1}H NMR (600 MHz, in CD$_3$OD) δ_H 7.41−7.53 (15H, m, MTPA-Ar), 5.41 (1H, br s, H-4), 5.30 (1H, br s, H-7), 5.19 (1H, br s, H-9), 4.13 (1H, d, *J* = 17.5 Hz, H-2a), 3.99 (1H, d, *J* = 17.5 Hz, H-2b), 3.69 (1H, m, H-10), 3.53 (3H, s, MTPA-OMe), 3.52 (3H, s, MTPA-OMe), 3.50 (3H, s, MTPA-OMe), 1.84 (1H, m, H-6a), 1.77 (1H, m, H-5a), 1.73 (1H, m, H-5b), 1.69 (1H, m, H-6b), 1.48 (1H, m, H-11a), 1.41 (1H, m, H-12a), 1.28 (1H, m, H-11b), 1.24 (1H, m, H-12b), 0.86 (3H, t, *J* = 7.1 Hz, H-13); HRESIMS *m/z* [M+Na]$^+$ 899.2452 (calcd. for C$_{42}$H$_{41}$F$_9$O$_{10}$Na, 899.2454).

R-MTPA Ester of **5** (**5b**): White amorphous solid. ^{1}H NMR (600 MHz, in CD$_3$OD) δ_H 7.43−7.54 (15H, m, MTPA-Ar), 5.41 (1H, br s, H-4), 5.20 (1H, s, H-7), 4.76 (1H, br s, H-9), 3.95 (1H, d, *J* = 17.6 Hz, H-2a), 3.75 (1H, ddd, *J* = 8.9, 5.0, 2.0 Hz, H-10), 3.68 (1H, dd, *J* = 17.6, 2.0 Hz, H-2b), 3.60 (3H, s, MTPA-OMe), 3.56 (3H, s, MTPA-OMe), 3.48 (3H, s, MTPA-OMe), 2.04 (1H, m, H-5a), 1.99 (1H, m, H-5b), 1.95 (1H, m, H-6a), 1.81 (1H, m, H-6b), 1.32 (1H, m, H-11a), 1.27 (1H, m, H-12a), 1.12 (1H, m,

H-12b), 0.95 (1H, m, H-11b), 0.82 (3H, t, J = 7.2 Hz, H-13); HRESIMS *m/z* [M+Na]$^+$ 899.2449 (calcd. for $C_{42}H_{41}F_9O_{10}Na$, 899.2454).

S-MTPA Ester of **6** (**6a**): White amorphous solid. ^{1}H NMR (600 MHz, in CD_3OD) δ_H 7.42–7.52 (15H, m, MTPA-Ar), 5.55 (1H, dd, J = 8.0, 6.0 Hz, H-4), 5.38 (1H, br s, H-7), 5.11 (1H, brs, H-9), 3.78 (1H, d, J = 16.9 Hz, H-2a), 3.65 (1H, m, H-10), 3.61 (1H, d, J = 17.0 Hz, H-2b), 3.54 (3H, s, MTPA-OMe), 3.52 (3H, s, MTPA-OMe), 3.48 (3H, s, MTPA-OMe), 2.11 (1H, m, H-5a), 1.98 (1H, m, H-6a), 1.95 (1H, m, H-6b), 1.61 (1H, m, H-5b), 1.29 (1H, m, H-11a), 1.25 (1H, m, H-12a), 1.20 (1H, m, H-12b), 1.15 (1H, m, H-11b), 0.81 (3H, t, J = 7.2 Hz, H-13); HRESIMS *m/z* [M+Na]$^+$ 899.2457 (calcd. for $C_{42}H_{41}F_9O_{10}Na$, 899.2454).

R-MTPA Ester of **6** (**6b**): white amorphous solid. ^{1}H NMR (600 MHz, in CD_3OD) δ_H 7.45–7.54 (15H, m, MTPA-Ar), 5.52 (1H, dd, J = 8.6, 5.3 Hz, H-4), 5.18 (1H, br s, H-7), 4.78 (1H, s, H-9), 4.05 (1H, d, J = 17.6 Hz, H-2a), 3.98 (1H, d, J = 17.4 Hz, H-2b), 3.84 (1H, m, H-10), 3.59 (3H, s, MTPA-OMe), 3.53 (3H, s, MTPA-OMe), 3.47 (3H, s, MTPA-OMe), 2.12 (1H, m, H-5a), 1.93 (1H, m, H-6a), 1.90 (1H, m, H-6b), 1.68 (1H, m, H-5b), 1.28 (1H, m, H-11a), 1.24 (1H, m, H-12a), 1.14 (1H, m, H-12b), 0.98 (1H, m, H-11b), 0.80 (3H, t, J = 7.3 Hz, H-13); HRESIMS *m/z* [M+Na]$^+$ 899.2453 (calcd. for $C_{42}H_{41}F_9O_{10}Na$, 899.2454).

3.7. X-Ray Crystallographic Analysis

Compound **5** was obtained as colorless crystals from acetone–ethyl acetate (1:4) using the vapor-exchanged method [11,19,20]. X-ray single-crystal diffraction data for **5** were collected at 293 K on a Rigaku Oxford Diffraction instrument using Cu Kα (λ = 1.54184) radiation. The structures were solved by direct methods using Olex2 software [21], and the non-hydrogen atoms were refined isotropically with SHELXL-2014 [22] using a full-matrix least squares procedure based on F^2. The hydrogen atoms were positioned according to the geometric calculation. Crystallographic data for the structures of **5** were deposited at the Cambridge Crystallographic Data Centre database (CCDC Number: 1890797).

Crystal data for **5**: $C_{12}H_{20}O_4$ (M = 228.28 g/mol), trigonal, space group P3$_1$ (no. 144), a = 14.9243(2)Å, b = 14.9243(2)Å, c = 4.49716(13)Å, V = 867.47(4)Å^3, Z = 3, T = 293 (10)K, μ(CuKα) = 0.798 mm^{-1}, $Dcalc$ = 1.311 g/cm^3, F (000) = 372.0. The final R_1 was 0.0397 (wR_2 = 0.1052) for 2082 unique reflections (I > 2σ (I)), and Flack = −0.01(11).

3.8. NO Inhibition Assay

Mouse monocyte-macrophages RAW 264.7 (ATCC TIB-71) were purchased from the Chinese Academy of Science. DMEM medium, penicillin, streptomycin, and fetal bovine serum were purchased from Invitrogen (N.Y., USA). Lipopolysaccharide (LPS), DMSO, 3-(4,5-dimethylthiazol-2-yl)-2,5-diphenyl-2H-tetrazolium bromide (MTT), and hydrocortisone were obtained from Sigma Co. RAW 264.7 cells were maintained in DMEM medium supplemented with penicillin, streptomycin (both 100 U/mL), and 10% heat-inactivated fetal bovine serum at 37 °C in a humidified incubator with 5% CO_2 and 95% air. RAW264.7 cells were passaged until they attained confluence. The cell concentration was adjusted to 5×10^5 cells/mL with 10% FBS DMEM medium, and 100 µL was seeded in each well of a 96-well plate that was maintained at 37 °C overnight. The supernatant was discarded, and the cells except for the blank control groups were treated with 100 µL of LPS DMEM (the concentration of LPS was 2 µg/mL or 5 µg/mL). After 2 h of incubation, blank and LPS model groups were treated with 100 µL of DMEM medium and the others were treated with DMEM medium containing various concentrations of test compounds for 24 h, respectively [16].

As a parameter of NO release, the nitrite concentration was measured in the supernatant of RAW 264.7 cells by the Griess reaction [16]. The inhibition rate was calculated and plotted versus test concentrations to afford the IC$_{50}$.

3.9. Cytotoxic Assay

The cytotoxicity of all of the compounds was measured by the MTT assay against the prostate cancer PC3 cell line. Tumor cell lines were seeded in 96-well plates (4000 per well in 100 µL). After 24 h of incubation, cells were treated with gradient concentrations (100 µM, 50 µM, 25 µM, 12.5 µM,

6.25 μM, 3.125 μM) for another 72 h. Afterwards, MTT solution (5.0 mg/mL in RPMI-1640 media, Sigma, St. Louis, MO, USA) was added (20 μL/well) and then plates were incubated for another 4 h at 37 °C. The compounds were dissolved in DMSO and a cell growth inhibition assay was performed as reported previously. The growth inhibitory abilities of the compounds were calculated and expressed using the IC$_{50}$ value by the Dose-Effect Analysis software. Doxorubicin (ADR) was used as a positive control.

3.10. Antibacterial Assay

The antibacterial activities of all compounds except for **4** and **7** were evaluated with *S. aureus*, *S. epidermidis*, *E. coli*, *M. albicans*, and *P. aeruginosa* using the Kirby−Bauer Diffusion method. Gentamicin, vancomycin, ampicillin, amphotericin B, and gentamicin served as the positive drugs, respectively.

The stock solution of compounds **1**, **2**, **3**, **5**, and **8** was prepared in methanol with a series of concentrations (25, 5.0, 1, and 0.2 mg/mL). The stock solution of compound **6** was prepared in methanol with a series of concentrations (5.0, 1, and 0.2 mg/mL). The positive control drugs gentamicin, vancomycin, and ampicillin were dissolved in purified water at a concentration of 500 ug/mL. Amphotericin B was dissolved in DMSO at a concentration of 100 ug/mL.

S. aureus, *S. epidermidis*, *E. coli*, *M. albicans*, and *P. aeruginosa* were activated in nutrient broth at 37 °C for 6~8 h with 200 rpm. The culture broth was poured on the surface of Malt Extract Broth (MEB) Agar (20 g MEB and 20 g agar in 1 L of water) plates inside the cabinet, making sure that there was a uniform distribution of cells on the plates. The location of the negative control (methanol), the positive drugs, and different contents of tested compounds (100 μg, 20 μg, 4 μg, and 0.8 μg for **1**, **2**, **3**, **5**, and **8**; 20 μg, 4 μg, and 0.8 μg for **6**) was labeled on the agar side of the plate and outside the lid. The discs were arranged so as to mimic their positions outside the lid and 4 μL of the corresponding concentrations of the tested compounds and methanol was added to the discs. The contents of the positive drugs gentamicin, ampicillin, and amphotericin B were 3 ug, 1.5 ug, and 0.35 ug, respectively. The discs were transferred from the lid to the agar plate using sterile forceps. Finally, the plates were placed in an incubator agar side up at 37 °C for 12 h and the inhibition zone was observed.

The estimations of the purity of compounds **1**–**8** for biological appraisals were 92.21%, 98.26%, 95.82%, 98.60%, 99.1%, 95.36%, and 99.05%, respectively.

4. Conclusions

With the aim of discovering structurally novel secondary metabolites, seven new polyketides (phomopsiketones D–G (**1**–**4**) and letendronols A–C (**5**–**7**)) were isolated from the marine endophytic fungus *Letendraea* sp. in 1/2 PDB medium. The structures and absolute configurations of the new compounds were sufficiently elucidated through HRESIMS, NMR, single-crystal X-ray diffraction, ECD calculation, and a modified version of Mosher's method. Compound **2** showed weak anti-inflammatory activity.

Author Contributions: Y.X. performed the experiments for the isolation, structure determination, and antimicrobial evaluation, and prepared the manuscript; H.L. performed the NO inhibition assay; Y.J. contributed to part of the structure determination; R.H. contributed to the preparation of the fermentation; W.D. performed the cytotoxic assay; T.Y. contributed to part of the isolation; P.W. and D.Z. conducted the isolation of strain 5XNZ4-2 and jointly supervised the research; J.X. supervised the research work and revised the manuscript. All authors have read and agreed to the published version of the manuscript.

Conflicts of Interest: The authors declare no conflict of interest.

References

1. Gudina, E.J.; Teixeira, J.A.; Rodrigues, L.R. Biosurfactants Produced by Marine Microorganisms with Therapeutic Applications. *Mar. Drugs* **2016**, *14*, 38. [CrossRef] [PubMed]

2. Tortorella, E.; Tedesco, P.; Palma Esposito, F.; January, G.G.; Fani, R.; Jaspars, M.; de Pascale, D. Antibiotics from Deep-Sea Microorganisms: Current Discoveries and Perspectives. *Mar. Drugs* **2018**, *16*, 355. [CrossRef] [PubMed]

3. Blunt, J.W.; Carroll, A.R.; Copp, B.R.; Davis, R.A.; Keyzers, R.A.; Prinsep, M.R. Marine natural products. *Nat. Prod. Rep.* **2018**, *35*, 8–53. [CrossRef] [PubMed]

4. Blunt, J.W.; Copp, B.R.; Keyzers, R.A.; Munro, M.H.; Prinsep, M.R. Marine natural products. *Nat. Prod. Rep.* **2016**, *33*, 382–431. [CrossRef] [PubMed]

5. Blunt, J.W.; Copp, B.R.; Keyzers, R.A.; Munro MH, G.; Prinsep, M.R. Marine natural products. *Nat. Prod. Rep.* **2017**, *34*, 235–294. [CrossRef]

6. Imhoff, J.F. Natural Products from Marine Fungi—Still an Underrepresented Resource. *Mar. Drugs* **2016**, *14*, 19. [CrossRef]

7. Huang, R.; Xu, Y.; Ye, B.; Ding, W.; Wang, P.; Xu, J. Letenketals A and B, two novel spirocyclic polyketides from a marine crab-derived Letendraea sp. fungus. *Phytochem. Lett.* **2019**, *30*, 165–168. [CrossRef]

8. Koizumi, F.; Takahashi, Y.; Ishiguro, H.; Tanaka, R.; Ohtaki, S.; Yoshida, M.; Nakanishi, S.; Ikeda, S.I. Structure elucidation of EI-1941-1 and -2, novel interleukin-1β converting enzyme inhibitors produced by *Farrowia* sp. E-1941. *Tetrahedron Lett.* **2004**, *45*, 7419–7422. [CrossRef]

9. Petrovic, A.G.; Navarro-Vazquez, A.; Lorenzo Alonso-Gomez, J. From Relative to Absolute Configuration of Complex Natural Products: Interplay between NMR, ECD, VCD, and ORD Assisted by ab initio Calculations. *Curr. Org. Chem.* **2010**, *14*, 1612–1628. [CrossRef]

10. Cerra, B.; Carotti, A.; Passer, D.; Sardella, R.; Moroni, G.; Di Michele, A.; Macchiarulo, A.; Pellicciar, R.; Gioielle, A. Exploiting Chemical Toolboxes for the Expedited Generation of Tetracyclic Quinolines as a Novel Class of PXR Agonists. *ACS Med. Chem. Lett.* **2019**, *10*, 677–681. [CrossRef]

11. Tang, J.W.; Wang, W.G.; Li, A.; Yan, B.C.; Chen, R.; Li, X.N.; Du, X.; Sun, H.D.; Pu, J.X. Polyketides from the endophytic fungus *Phomopsis* sp. sh917 by using the one strain/many compounds strategy. *Tetrahedron* **2017**, *73*, 3577–3584. [CrossRef]

12. Fischer, T.C.; Cerra, B.; Fink, M.J.; Rudroff, F.; Horkel, E.; Mihovilovic, M.D. First Total Synthesis of Piperenol B and Configuration Revision of the Enantiomers Piperenol B and Uvarirufol A. *Eur. J. Org. Chem.* **2015**, 1464–1471. [CrossRef]

13. Seco, J.M.; Quinoa, E.; Riguera, R. Assignment of the Absolute Configuration of Polyfunctional Compounds by NMR Using Chiral Derivatizing Agents. *Chem. Rev.* **2012**, *112*, 4603–4641. [CrossRef] [PubMed]

14. Khamthong, N.; Rukachaisirikul, V.; Phongpaichit, S.; Preedanon, S.; Sakayaroj, J. Bioactive polyketides from the sea fan-derived fungus Penicillium citrinum PSU-F51. *Tetrahedron* **2012**, *68*, 8245–8250. [CrossRef]

15. Mullapudi, V.; Ramana, C.V. The Total Synthesis and Structural Assignment of Hexaketide Xylarinol B and its C1'-Epimer. *Asian J. Org. Chem.* **2016**, *5*, 417–422. [CrossRef]

16. Han, J.J.; Chen, Y.H.; Bao, L.; Yang, X.L.; Liu, D.; Li, S.J.; Zhao, F.; Liu, H. Anti-inflammatory and cytotoxic cyathane diterpenoids from the medicinal fungus Cyathus africanus. *Fitoterapia* **2013**, *84*, 22–31. [CrossRef]

17. Li, X.; Zhao, Z.; Ding, W.; Ye, B.; Wang, P.; Xu, J. Aspochalazine A, a Novel Polycyclic Aspochalasin from the Fungus *Aspergillus* sp. Z4. *Tetrahedron Lett.* **2017**, *58*, 2405–2408. [CrossRef]

18. Li, Q.; Zhu, R.; Yi, W.; Chai, W.; Zhang, Z.; Lian, X.Y. Peniciphenalenins A–F from the culture of a marine-associated fungus *Penicillium* sp. ZZ901. *Phytochemistry* **2018**, *152*, 53–60. [CrossRef]

19. Van der Sluis, P.; Hezemans, A.M.F.; Kroon, J. Crystallization of low-molecular-weight organic compounds for X-ray crystallography. *J. Appl. Crystallogr.* **1989**, *22*, 340–344. [CrossRef]

20. Spingler, B.; Schnidrig, S.; Todorova, T.; Wild, F. Some thoughts about the single crystal growth of small molecules. *CrystEngComm* **2012**, *14*, 751–757. [CrossRef]

21. Dolomanov, O.V.; Bourhis, L.J.; Gildea, R.J.; Howard, J.A.K.; Puschmann, H. OLEX2: A complete structure solution, refinement and analysis program. *J. Appl. Crystallogr.* **2009**, *42*, 339–341. [CrossRef]

22. Kratzert, D.; Holstein, J.J.; Krossing, I. DSR: Enhanced modelling and refinement of disordered structures with SHELXL. *J. Appl. Crystallogr.* **2015**, *48*, 933–938. [CrossRef] [PubMed]